separations

MDPI

Article

Isolation, Structural Characterization, and In Vitro Antioxidant Activity of Polysaccharides from *Cynanchum auriculatum* Royle ex Wight

Hequan Zhu, Mustapha Muhammad Nasiru, Sijia Jiang, Yuetao Sun, Dan Liu and Chunyang Li *

Institute of Agro-Product Processing, Jiangsu Academy of Agricultural Sciences, Nanjing 210014, China; zhuhequanzz@163.com (H.Z.); nasirumm@jaas.ac.cn (M.M.N.); jiang_ang411@163.com (S.J.); sven_sun1110@163.com (Y.S.); liud870@163.com (D.L.)
* Correspondence: lichunyang968@126.com

Abstract

A novel polysaccharide from *Cynanchum auriculatum* Royle ex Wight was isolated, structurally characterized, and its antioxidant activity was evaluated. The crude extract was purified by ion exchange and size exclusion chromatography to obtain a homogeneous fraction, CAP2-1. CAP2-1 displayed a weight-average molecular mass of 184.17 kDa and is mainly composed of galactose, arabinose, and galacturonic acid. Structural analysis revealed that CAP2-1 is a highly branched acidic arabinogalactan-type polysaccharide with a backbone of →6)-β-D-Galp-(1→, →3,6)-β-D-Galp-(1→, and →4)-α-D-GalpA-(1→ units, and side chains enriched in α-L-arabino furanose residues. Ultrasonic degradation produced a lower-molecular-weight derivative, UCAP2-1, which exhibited significantly stronger free radical scavenging ability compared with CAP2-1 ($p < 0.01$). These findings suggest that molecular weight reduction enhances antioxidant properties by improving electron-donating capacity and accessibility to reactive sites. This study reveals the structure–antioxidant relationship of CAP2-1 and UCAP2-1 and highlights UCAP2-1 as a promising natural antioxidant.

Keywords: *Cynanchum auriculatum* Royle ex Wight; polysaccharide; structural characterization; antioxidant activity; structure–activity relationship

1. Introduction

Human health has long been fundamentally challenged by the lethal effects of oxidative stress [1]. Oxidative stress refers to a disrupted redox homeostasis caused by excessive accumulation of reactive oxygen species (ROS) beyond the capacity of cellular antioxidant systems [2]. This pathological condition is a central mechanism driving the initiation and progression of numerous chronic diseases that burden global populations [3], such as cardiovascular disorders [4], neurodegenerative conditions [5], diabetes mellitus [6], and various cancers [7]. Consequently, the pursuit of effective antioxidants to mitigate oxidative damage represents a key frontier in biomedical research for disease prevention and management. Natural antioxidants, especially phytochemicals, are widely regarded as safer and more sustainable alternatives to synthetic compounds [8]. Notably, polysaccharides of natural origin are increasingly recognized for their bioactivity and potential functional application, exhibiting a remarkable array of therapeutic properties, including antioxidant [9], anti-inflammatory [10], immunomodulatory [11], and anticancer [12] activities.

Check for updates

Academic Editor: Victoria Samanidou

Received: 17 December 2025
Revised: 18 January 2026
Accepted: 21 January 2026
Published: 23 January 2026

Copyright: © 2026 by the authors. Licensee MDPI, Basel, Switzerland. This article is an open access article distributed under the terms and conditions of the Creative Commons Attribution (CC BY) license.

Polysaccharides, as essential biological macromolecules alongside nucleic acids and proteins, have historically received less systematic investigation than their counterparts. While foundational research on nucleic acids and proteins dates back centuries, dedicated scientific inquiry into polysaccharides emerged only in the last century and has expanded significantly in recent decades. Research on polysaccharides spans several critical domains, encompassing their biological activities, structural characterization, structure-activity relationships (SAR), modification strategies, and potential applications in biomaterials [13–15]. Among these, biological activity, structural characterization, and their interrelationship through SAR constitute the most fundamental and pivotal research focus. These core aspects provide the essential basis for elucidating the underlying mechanisms of polysaccharide biological activity and for guiding their future development across various applied contexts.

Polysaccharides isolated from diverse plant sources have demonstrated notable antioxidant properties. For instance, ginseng polysaccharides demonstrate potent antioxidant effects [13]; *Houttuynia cordata* polysaccharides show significant anti-colitis activity [14]; lettuce polysaccharides display immunomodulatory functions [15]; and *Sargassum duplicatum* polysaccharides exhibit notable anticancer activity in vitro. Moreover, this bioactivity of polysaccharides largely depends on their molecular structural conformation. In particular, polysaccharides with lower molecular weight and more complex branching tend to exhibit more potent antioxidant and biological activities [16]. For example, microwave/ultrasonic-assisted extraction yielded a 89 kDa polysaccharide from *Pleurotus ferulae* with superior antioxidant activity relative to conventional methods [17].

Additionally, the antioxidant bioactivity of natural polysaccharides is closely associated with glycosidic linkage configurations and monosaccharide composition. Previous studies have indicated that specific monosaccharides play critical roles in determining antioxidant potential. For example, in *Lentinula edodes* polysaccharides, rhamnose content was identified as a key factor influencing antioxidant properties. At the same time, arabinose 1→4 and mannose 1→2 linkages within side chains were significantly correlated with reducing capacity [18]. Notably, the structural features of polysaccharides are highly dependent on the extraction and purification approaches employed [19–21]. Different extraction strategies significantly influence key structural features. Likewise, the subsequent purification steps are crucial for ensuring homogeneity and defining the final polysaccharide structure. Furthermore, various analytical techniques, including high-performance liquid chromatography (HPLC), gas chromatography (GC), fourier-transform infrared spectroscopy (FT-IR), and nuclear magnetic resonance (NMR) spectroscopy, have been employed to elucidate the molecular weight and structural characteristics of polysaccharides [22]. Although the SAR of polysaccharides has been characterized in several plant species [23], the biological activities, structural attributes, and corresponding SAR of polysaccharides from many others—including *Cynanchum auriculatum* Royle ex Wight (*C. auriculatum*)—remain insufficiently investigated and are yet to be comprehensively elucidated.

C. auriculatum is a traditional plant used in both medicine and food, with a long history of consumption across many Asian countries, including China, India, Japan, and Korea [24]. *C. auriculatum* is well-regarded for its diverse bioactivities, including antitumor [25], antioxidant [26], anti-diabetic, and gut microbiota-modulating effects [27]. Consequently, the bioactive compounds derived from this plant, such as phenols, flavonoids, and steroidal glycosides, have attracted significant interest from researchers [28–30], with C-21 steroidal glycosides being the most extensively studied. C-21 Steroidal glycosides exert significant hepatoprotective effects through upregulating the Nrf2/HO-1 pathway while concurrently inhibiting NF-κB–dependent inflammatory responses, thereby mitigating oxidative stress triggered by H_2O_2 and subsequent pro-inflammatory cytokine production

in L-02 hepatocytes [30]. Beyond cytoprotection, six distinct C-21 steroidal glycosides demonstrate selective antineoplastic activity in vitro and in vivo, triggering apoptosis and markedly restraining H22 tumor growth [31]. However, research on *C. auriculatum* polysaccharides remain limited, and neither their detailed structural features nor their structure–activity relationships, particularly with respect to antioxidant activity, have been extensively investigated.

In the present study, polysaccharides from *C. auriculatum* were isolated, and a novel purified fraction (CAP2-1) together with its ultrasonic degradation product (UCAP2-1) was obtained. The main objective of this work was to elucidate the structural characteristics of CAP2-1 and to investigate how ultrasonic degradation influences its antioxidant activity. By integrating structural analysis and in vitro antioxidant evaluation, this study aims to clarify the structure–activity relationship of *C. auriculatum* polysaccharides and assess their potential application as natural antioxidants.

2. Materials and Methods

2.1. Materials and Chemicals

The *C. auriculatum* was purchased from Yancheng Guolao Shouwu Science and Technology Development Co., Ltd. (Yancheng, China).

Phenol, sulfuric acid, trifluoroacetic acid, acetic anhydride and NaCl were of analytical grade and obtained from Sinopharm Chemical Reagent Co., Ltd. (Shanghai, China). m-Hydroxybiphenyl, sodium tetraborate, galacturonic acid, potassium bromide, sodium borodeuteride, pyridine, and dimethyl sulfoxide were purchased from Shanghai Aladdin Bio-Technology Co., Ltd. (Shanghai, China). Iodomethane was purchased from Anhui Zesheng Technology Co., Ltd. (Hefei, China). DEAE-cellulose-52, Sephadex G-150 amylase, and amyloglucosidase were purchased from Yuanye Bio-Technology Co., Ltd. (Shanghai, China). Twelve monosaccharide standards and dextran series standards, 2,2-azino-bis (3-ethylbenzothiazoline-6-sulfonic acid) diammonium salt (ABTS), 1,1-diphenyl-2-picrylhydrazyl (DPPH), and hydrogen peroxide (H_2O_2) were all purchased from Sigma Chemical Co. (St. Louis, MO, USA).

2.2. Preparation of CAP

The CAPs were isolated and purified as described in our previous study [24]. The root of *C. auriculatum* Royle ex Wight was air-dried in an oven (at 50 °C for 24 h). The dried roots were ground and sieved (100 mesh) to obtain a fine powder. The Lipids and pigments were removed by three extractions with 80% ethanol at 50 °C for 3 h. After drying at 50 °C for 48 h, the degreased powder (300 g) was pretreated with distilled water (1:17, w/v) containing α-amylase (10 U/g) at 60 °C for 30 min to reduce extract viscosity. Then the temperature was elevated to 92 °C for 3 h. The supernatant was separated and combined by centrifugation at 5000× g for 10 min using GTR420 centrifuge (Hunan Kecheng Instrument and Equipment Co., Ltd., Changsha, China). α-Amylase and amyloglucosidase were used to remove starch. The filtrate was concentrated to one-twentieth of its original volume under reduced pressure through a rotary evaporator (RE-52AA, Yarong Co., Ltd., Shanghai, China). It was removed by means of the Sevag method [32]. The resulting solution was then precipitated with four volumes of ethanol overnight, and the precipitate was collected by centrifugation at 5000× g for 10 min and washed three times with 80% (v/v) ethanol. After redissolution, dialysis and freeze-drying, crude CAPs were obtained.

A total of 500 mg of crude CAPs was dissolved in 100 mL of deionized water, and after centrifugation, the solution was loaded onto a DEAE-cellulose DE-52 column (2.6 × 60 cm) (Yuanye Bio-Technology Co., Ltd., Shanghai, China). Sequential elution was performed with deionized water and 0.1–0.5 mol/L NaCl at 2.0 mL/min. The absorbance of each eluted

fraction was determined at 490 nm by the phenol–sulfuric acid assay [33]. The significant fractions were collected, and then were dialyzed, lyophilized, purified by Sephadex G-150 gel filtration (1.0 × 60 cm) (Yuanye Bio-Technology Co., Ltd., Shanghai, China). The major polysaccharide fraction (5 mg/mL) was eluted with deionized water at 0.2 mL/min, and the purified fractions were collected, dialyzed, and lyophilized.

The purified polysaccharide was subjected to ultrasonic degradation using an ultrasonic cell disruptor. The polysaccharide was dissolved in ultrapure water to obtain a 1 mg/mL solution, which was then placed in an JY88-PRO ultrasonic cell crusher (Ningbo Scientz Biotechnology Co., Ltd., Ningbo, China). The solution was sonicated at 400 W and 20 kHz for 1 h in an ice bath. After ultrasonic treatment, the degraded polysaccharide was lyophilized and stored for further analysis.

2.3. Homogeneity and Molecular Weight Analysis

High performance size exclusion chromatography (HPSEC) was used to assess the homogeneity and Mw distribution of the polysaccharide fraction [34]. The dextran standards were prepared at 1 mg/mL in the mobile phase and filtered through a 0.45 μm membrane, and injected sequentially. The retention times were recorded and used to construct a calibration curve. The polysaccharide sample was prepared using the same procedure. The Mw of the sample was determined using the calibration curve. The chromatographic analyses were conducted on a Waters 1525 HPLC platform fitted (Waters, Milford, MA, USA) fitted with column (300 × 7.8 mm, 2 μm) and a Waters 2414 refractive index detector. A 0.1 mol/L $NaNO_3$ solution served as the mobile phase at 0.9 mL/min, while the column was maintained at 45 °C.

2.4. FT-IR Spectroscopy

The FT-IR spectra were acquired for the polysaccharide samples to identify characteristic functional groups. For FT-IR analysis, a small amount of the dried polysaccharide (≈2 mg) was intimately combined with dried KBr (200 mg) and mechanically pulverized in an agate mortar until a uniform powder was obtained. After pelletization under hydraulic pressure, spectral data were acquired across the 400–4000 cm^{-1} range.

2.5. Monosaccharide Composition Analysis

The ion chromatography (ICS) was employed to characterize the monosaccharide composition of the polysaccharide, as previously reported by Yang et al. [35], with minor modifications. In brief, 5 mg of the polysaccharide sample was accurately weighed into chromatographic vials, subsequently treated with freshly prepared 2 mol/L trifluoroacetic acid (TFA). The samples hydrolysis reaction proceeded at 121 °C for 2 h in an oil bath. After hydrolysis, TFA was removed by nitrogen evaporation, and the residue was washed three times with methanol, each wash followed by evaporation to dryness to eliminate residual acid. After reconstitution in deionized water and filtration, the hydrolysates were analyzed using ICS. ICS analysis was performed on a Thermo ICS-5000+ ion chromatography system (Thermo Scientific, Waltham, MA, USA) fitted with an electrochemical detector and a Dionex™ CarboPac™ PA10 column (250 × 4.0 mm, 10 μm) (Thermo Scientific, Waltham, MA, USA). The injection volume was 20 μL, and the column temperature was maintained at 30 °C. Mobile phase A was deionized water, and mobile phase B was 100 mM NaOH. The chromatographic separation was carried out under a gradient elution program consisting of 97.5% A/2.5% B (0–30 min), 80% A/20% B (30–45 min), and 60% A/40% B (45–60 min).

2.6. Methylation Analysis

Glycosidic linkage patterns of the polysaccharide were elucidated by methylation analysis. The sample was first premethylated with CH_3I and powdered NaOH in DMSO, as

described previously [36]. Successful methylation was verified by the absence of hydroxyl absorption in the 3100–3700 cm^{-1} region of the FT-IR spectrum, as previously reported [37]. The completely methylated polysaccharide was then hydrolyzed in 2 M TFA at 120 °C for 2 h. After reduction with $NaBD_4$ at 50 °C for 2 h, residual boric acid was eliminated by repeated methanol co-evaporation. Acetylation of the partially methylated monosaccharides was performed with acetic anhydride and pyridine (1:1, *v*/*v*) at 120 °C for 30 min. The derived partially methylated alditol acetates (PMAAs) were characterized by GC–MS using an Agilent 7000D system (Agilent, Santa Clara, CA, USA) fitted with an HP-5MS capillary column (30 m × 0.25 mm × 0.25 μm) (Agilent, Santa Clara, CA, USA).

2.7. NMR Spectroscopy

To obtain a comprehensive understanding of the structural characteristics of the purified polysaccharide, NMR spectroscopy was performed [38]. The polysaccharide was solubilized in D_2O and repeatedly lyophilized three times to ensure complete deuterium exchange. After deuterium exchange, 50 mg of the sample was re-dissolved in 0.5 mL of D_2O and transferred to an NMR tube for analysis. ^1H NMR, ^{13}C NMR, ^1H–^1H correlation spectroscopy (^1H–^1H COSY), heteronuclear single quantum coherence (HSQC), and heteronuclear multiple bond correlation (HMBC) were acquired on a Bruker DRX-600 NMR instrument (Bruker, Ettlingen, Germany).

2.8. Assay of Antioxidant Activity In Vitro

2.8.1. DPPH Radical Scavenging Activity

The DPPH radical scavenging activity of the polysaccharide samples was evaluated as described in a prior study [39], with minor adjustments. A series of polysaccharide solutions (0.1–2.5 mg/mL) was prepared, and vitamin C (Vc) within the same concentration range was employed as the reference antioxidant. After reaction with the DPPH solution, absorbance was measured, and the radical scavenging activity was determined using the equation presented below:

$$\text{Scavenging capacity on DPPH radical (\%)} = [1 - (A_{sample} - A_{control})/A_{blank}] \times 100 \quad (1)$$

where A_{sample}, $A_{control}$, and A_{blank} correspond to the absorbance of the polysaccharide–DPPH mixture, polysaccharide solution without DPPH, and DPPH solution alone, respectively.

2.8.2. ABTS Radical Scavenging Activity

The ability of the polysaccharide samples to scavenge ABTS radicals was determined according to an established method [40] with slight modifications. A series of polysaccharide solutions (0.1–2.5 mg/mL) was prepared, and Vc within the same concentration range was employed as the reference antioxidant. After reaction with the ABTS working solution, absorbance values were recorded, and the radical scavenging activity was determined using the equation presented below:

$$\text{Scavenging capacity on ABTS radical (\%)} = [1 - (A_{sample} - A_{control})/A_{blank}] \times 100 \quad (2)$$

where A_{sample}, $A_{control}$, and A_{blank} correspond to the absorbance of the polysaccharide–ABTS mixture, polysaccharide solution without ABTS, and ABTS solution alone, respectively.

2.8.3. Hydroxyl Radical Scavenging Activity

The ability of the polysaccharide samples to scavenge hydroxyl radicals was assessed based on an established method [41], with minor modifications. A series of polysaccharide solutions (0.1–2.5 mg/mL) was prepared, and Vc at the same concentrations was employed as the reference antioxidant. After reaction with the hydroxyl radical-generating system,

the absorbance values were recorded, and the scavenging activity was determined using the equation presented below:

$$\text{Hydroxyl scavenging activity (\%)} = [1 - (A_{sample} - A_{control})/A_{blank}] \times 100 \quad (3)$$

where A_{sample}, $A_{control}$, and A_{blank} correspond to the absorbance of the reaction mixture, sample solution without hydroxyl radicals, and hydroxyl radical system alone, respectively.

2.9. Statistical Analysis

Each experiment was repeated three times, with results reported as as mean ± standard deviation (SD). Statistical analyses were conducted using Origin 2022 (OriginLab, Northampton, MA, USA). Statistical differences among groups were assessed using one-way analysis of variance (ANOVA), followed by Duncan's multiple range test. Statistical significance was defined at $p < 0.05$.

3. Results and Discussion

3.1. Purification of CAPs

The crude polysaccharides (500 mg) extracted from *C. auriculatum* were initially subjected to fractionation using a DEAE-cellulose-52 weak anion-exchange column (Yuanye Bio-Technology Co., Ltd., Shanghai, China). As illustrated in Figure 1a, four polysaccharide fractions were obtained according to their elution profiles: a neutral fraction (CAPW), eluted with distilled water, and three acidic fractions (CAP1, CAP2, and CAP3), eluted sequentially with NaCl solutions of increasing ionic strength. Each fraction was collected, dialyzed, and lyophilized, yielding 20.7%, 3.3%, 22.5%, and 6.0% (*w*/*w*), respectively. Among these, CAP2 exhibited both a relatively high yield and a well-defined elution peak; therefore, it was selected for further purification by Sephadex G-150 gel filtration chromatography (Yuanye Bio-Technology Co., Ltd., Shanghai, China). As presented in Figure 1b, CAP2 was resolved into two individual components, designated CAP2-1 and CAP2-2. After dialysis and lyophilization, the respective yields (*w*/*w*) of CAP2-1 and CAP2-2 were 19% and 3%.

3.2. The Mw of CAP2-1 and UCAP2-1

CAP2-1 was subjected to ultrasonic treatment, yielding its ultrasonically degraded derivative, designated as UCAP2-1. The average Mw and homogeneity of CAP2-1 and UCAP2-1 were analyzed by HPSEC. As shown in Figure 1c, CAP2-1 exhibited a single, symmetrical, and narrow chromatographic peak, indicating a high degree of homogeneity. The result indicated that CAP2-1 exhibited an Mw of 184.17 kDa, confirming that the fraction obtained was a highly purified polysaccharide. In contrast, the HPSEC chromatogram of UCAP2-1 (Figure 1d) showed two distinct peaks at 77.81 kDa and 1.69 kDa, accounting for 3.54% and 96.46% of the peak area, respectively. These results demonstrate that ultrasonic treatment effectively depolymerized CAP2-1, yielding a mixture dominated by a low-molecular-weight component.

3.3. FT-IR Analysis of CAP2-1

Figure 2a presents the FT-IR spectrum of CAP2-1, displayed several characteristic absorption bands indicative of its polysaccharide nature. The FT-IR spectrum exhibited a broad band at 3408 cm^{-1} corresponding to O–H stretching and a peak at 2932 cm^{-1} associated with C–H stretching, which are typical signatures of carbohydrates [42]. The absorption band observed at 1735 cm^{-1} was attributed to C=O stretching vibrations of esterified or acetyl groups [43]. In addition, the peak observed at 1632 cm^{-1} was associated with the O–H bending vibration of bound water commonly retained within polysaccharide matrices [44]. A signal at 1421 cm^{-1} corresponding to –COOH stretching suggested that

CAP2-1 contains uronic acid residues [45]. Furthermore, the absorption at 1251 cm^{-1} was attributed to the C–O–C stretching vibration in furanose ring ether linkages [46]. In contrast, the strong peak at 1073 cm^{-1} corresponded to pyranose ring vibrations, indicative of hexose units [47].

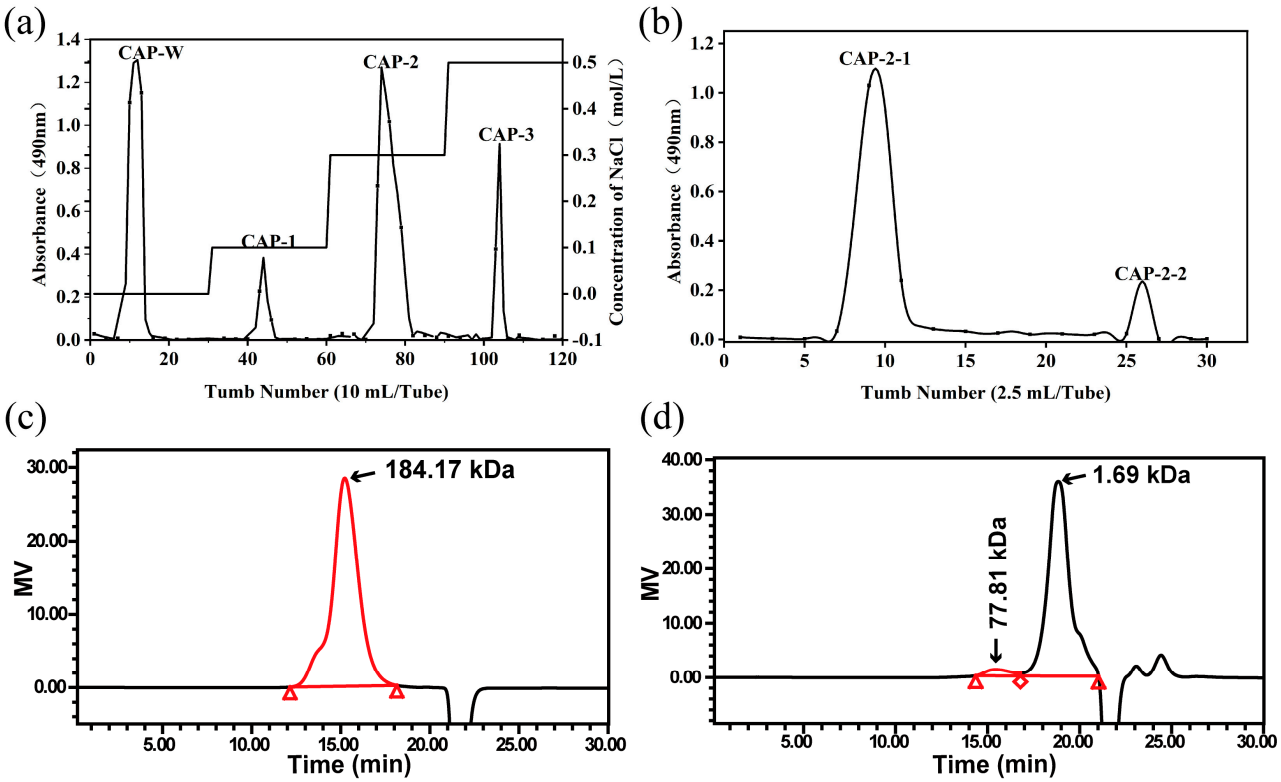


Figure 1. (**a**) DEAE-cellulose-52 elution curve of crude CAPs; (**b**) Sephadex G-150 column elution curve of crude CAP-2; (**c**) The HPSEC chromatogram of CAP2-1; (**d**) The HPSEC chromatogram of UCAP2-1.

3.4. Monosaccharide Composition of CAP2-1

The ion chromatographic analysis following acid hydrolysis revealed the monosaccharide composition of CAP2-1 (Figure 2b). As shown in Figure 2b, CAP2-1 was composed primarily of rhamnose, arabinose, galactose, and galacturonic acid. Quantitative analysis revealed that these monosaccharides accounted for 9.73% ± 0.03%, 35.31% ± 0.12%, 31.28% ± 0.08%, and 23.68% ± 0.05% of the total molar ratio, respectively. The substantial proportion of galacturonic acid indicates that CAP2-1 is an acidic polysaccharide [48]. Moreover, the presence of both arabinose and galactose suggests that CAP2-1 is likely an arabinogalactan-type polysaccharide, a structural feature commonly associated with plant-derived acidic heteropolysaccharides [49,50]. Such compositions are often linked to specific biological activities, including antioxidant and immunomodulatory functions, providing a structural basis for the functional properties investigated in subsequent assays [49,50].

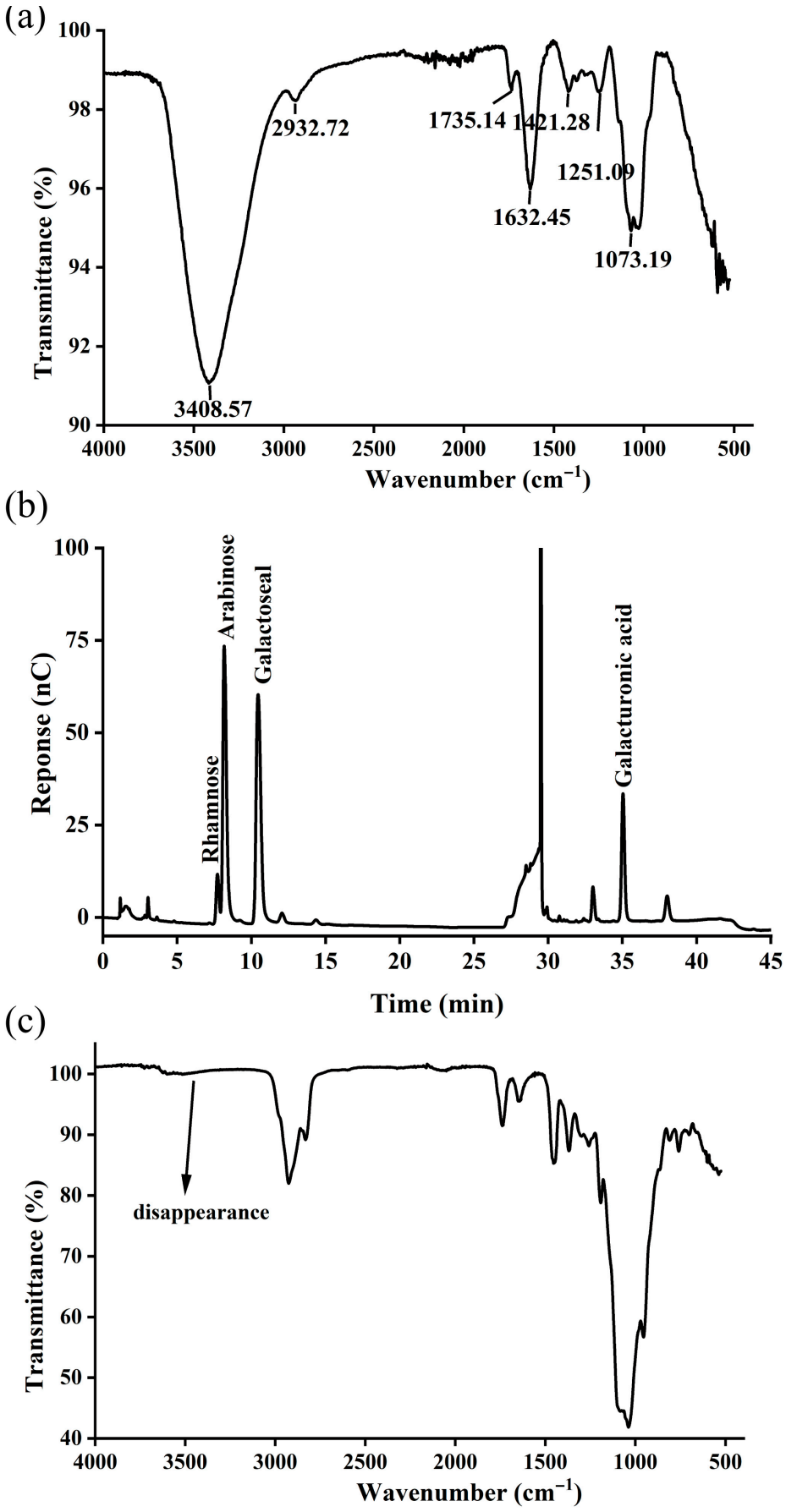


Figure 2. (**a**) FT-IR spectrum of CAP2-1; (**b**) The ICS chromatogram of CAP2-1; (**c**) FT-IR spectrum for methylated CAP2-1.

3.5. Linkage Feature of CAP2-1

Methylation analysis was conducted to elucidate the glycosidic linkage patterns of CAP2-1. The disappearance of the broad O–H stretching band at 3100–3700 cm^{-1} in the FT-IR spectrum confirmed complete methylation (Figure 2c), indicating replacement of hydroxyl groups with methoxy groups (–OCH_3) [51]. The partially methylated alditol acetates (PMAAs) generated after hydrolysis, reduction, and acetylation were identified by their characteristic mass spectrometric fragmentation patterns reported in the literature [52–54], and the results are summarized in Table 1. The major methylated residues detected in CAP2-1 included 2,3,5-Me_3-Araf, 2,3-Me_2-Araf, 2-Me-Araf, 2,3,4,6-Me_4-Galp, 2,3,4-Me_3-Galp, 2,4-Me_2-Galp, 2,3,6-Me_3-Galp, and 2,4-Me_2-Rhap, with molar ratios of 2.13, 1.76, 0.86, 0.99, 2.25, 0.89, 1.57, and 0.53, respectively. These methylation products indicate the presence of α-Araf-(1→, →5)-α-Araf-(1→, →3,5)-α-Araf-(1→, α-Galp-(1→, →6)-β-Galp-(1→, →3,6)-β-Galp-(1→, →4)-α-GalpA-(1→, and →3)-α-Rhap-(1→ linkages in the polysaccharide backbone. The substitution patterns further suggest that branching in CAP2-1 occurs primarily at O-6 of →3,6)-β-Galp-(1→ residues and at O-5 of →3,5)-α-Araf-(1→ residues. This branching profile is characteristic of arabinogalactan-type acidic heteropolysaccharides. Moreover, the relative proportions of Ara, Gal, and GalA residues inferred from methylation analysis were consistent with their molar ratios obtained from monosaccharide composition analysis, supporting the reliability of the structural deductions.

Table 1. Methylation analysis results of CAP2-1.

Methylated Sugars	Linkages	Major Mass Fragments (*m*/*z*)	Molar Ratio
2,3,5-Me_3-Araf	α-Araf-(1→	43, 71, 87, 102, 118, 129, 161	2.13
2,3-Me_2-Araf	→5)-α-Araf-(1→	43, 87, 102, 118, 129, 189	1.76
2-Me-Araf	→3,5)-α-Araf-(1→	43, 88, 101, 117, 130, 143, 190	0.86
2,3,4,6-Me_4-Galp	α-Galp-(1→	43, 45, 71, 87, 102, 118, 129, 145, 161, 205	0.99
2,3,4-Me_3-Galp	→6)-β-Galp-(1→	43, 45, 87, 99, 102, 113, 118, 129, 162, 173, 233	2.25
2,4-Me_2-Galp	→3,6)-β-Galp-(1→	43, 87, 101, 118, 129, 160, 234	0.89
2,3,6-Me_3-Galp	→4)-α-GalpA-(1→	43, 71, 87, 99, 102, 113, 118, 129, 131, 162, 173, 233	1.57
2,4-Me-Rhap	→3)-α-Rhap-(1→	43, 57, 71, 87, 99, 102, 118, 129, 162, 189, 233	0.53

3.6. NMR Spectral Analysis of CAP2-1

The structural features of CAP2-1 were further investigated by 1D and 2D NMR analyses (Figure 3), and the summary of the chemical shift assignments for CAP2-1 is presented in Table 2. In the ^1H NMR spectrum (Figure 3a), eight anomeric proton signals were observed at δ 5.18, 5.17, 5.11, 5.08, 5.04, 5.01, 4.56, and 4.53 ppm, indicating the presence of multiple glycosidic linkages. Proton signals corresponding to H-2–H-6 of sugar residues were distributed between δ 3.20–4.50 ppm, which is typical for polysaccharides; however, precise assignment of these signals was not feasible based solely on the ^1H spectrum [55]. The residual signal of D_2O appeared at δ 4.71 ppm.

As shown in Figure 3b, the ^{13}C NMR spectrum revealed eight anomeric carbon resonances at δ 109.32, 107.60, 107.06, 106.55, 104.50, 103.28, 102.76, and 100.86 ppm further confirmed the presence of eight distinct sugar residues. The remaining carbon signals were located between δ 60.38–84.22 ppm, corresponding to C-2–C-6 carbons of the various monosaccharide units.

Detailed assignments of proton and carbon signals were achieved by combining COSY, HSQC, and HMBC spectra with the methylation results and previously reported data [52–54]. In the COSY spectrum (Figure 3c), sequential correlations such as δ 5.11/4.09 (H-1/H-2), δ 4.09/3.88 (H-2/H-3), δ 3.88/3.77 (H-3/H-4), and δ 3.77/3.54, 3.50 (H-4/H-5a, H-5b) enabled the assignment of residue A, with analogous correlations observed for residues B–H. The HSQC spectrum (Figure 3d) revealed direct ^1H–^{13}C correlations for

anomeric pairs, assigning H-1/C-1 signals for residues A–H at δ 5.11/104.50, 5.18/107.60, 5.17/107.06, 5.04/103.28, 4.56/109.32, 4.03/102.76, 5.01/106.55, and 5.08/100.86 ppm, respectively. Cross-peaks for H-2/C-2 through H-6/C-6 were similarly identified. HMBC analysis (Figure 3e) provided key long-range correlations that established the linkage pattern of CAP2-1. Specially, the crossing signal at δ 4.56/70.18 ppm, δ 4.56/77.82 ppm, δ 4.56/69.45 ppm, δ 4.06/107.60 ppm, δ 3.37/107.10 ppm, δ 3.83/107.10 ppm, δ 3.88/107.10 ppm, δ 3.87/107.10 ppm, δ 3.88/107.60 ppm, δ 3.87/107.60 ppm, δ 3.52/109.32 ppm, δ 3.52/102.76 ppm can be assigned to $E_{H\text{-}1}/H_{C\text{-}3}$, $E_{H\text{-}1}/G_{C\text{-}4}$, $E_{H\text{-}1}/F_{C\text{-}6}$, $C_{H\text{-}3}/A_{C\text{-}1}$, $B_{H\text{-}5a}/C_{C\text{-}1}$, $B_{H\text{-}5b}/C_{C\text{-}1}$, $C_{H\text{-}5a}/C_{C\text{-}1}$, $C_{H\text{-}5b}/C_{C\text{-}1}$, $C_{H\text{-}5a}/A_{C\text{-}1}$, $C_{H\text{-}5b}/A_{C\text{-}1}$, $F_{H\text{-}3}/B_{C\text{-}1}$, $F_{H\text{-}3}/D_{C\text{-}1}$, meaning the existence of E-(1→3)-H, E-(1→4)-G, E-(1→6)-F, A-(1→3)-C, C-(1→5)-B, C-(1→5)-C, A-(1→5)-C, B-(1→3)-F and D-(1→3)-F linkages in CAP2-1.

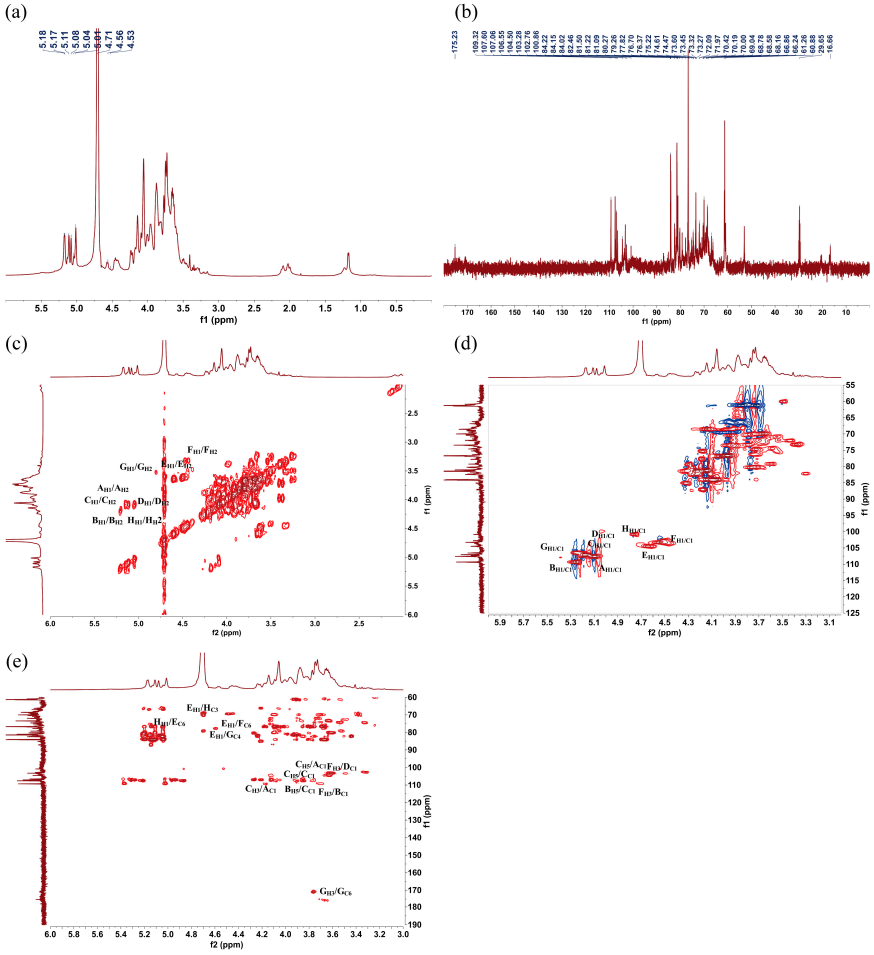


Figure 3. (**a**) ^{1}H NMR of CAP2-1; (**b**) ^{13}C NMR of CAP2-1; (**c**) ^{1}H-^{1}H COSY of CAP2-1; (**d**) HSQC of CAP2-1; (**e**) HMBC of CAP2-1.

Table 2. Chemical shifts of ^{1}H and ^{13}C NMR signals for the CAP2-1.

	Residues	C-1/H-1	C-2/H-2	C-3/H-3	C-4/H-4	C-5/H-5ab	C-6/H-6ab
A	α-L-Araf-(1→	107.60/5.11	81.09/4.09	76.70/3.88	81.45/3.77	61.26/3.54 or 3.50	
B	→5)-α-L-Araf-(1→	109.32/5.18	82.46/4.18	77.80/3.98	81.50/4.08	68.58/3.37 or 3.83	
C	→3,5)-α-L-Araf-1→	107.06/5.17	81.22/4.17	84.15/4.06	81.40/4.26	68.58/3.88 or 3.87	
D	α-D-Galp-(1→	102.76/5.04	74.61/4.00	76.37/3.90	73.27/3.77	75.22/3.54	73.32/3.33 or 3.21
E	→6)-β-D-Galp-(1→	104.50/4.56	74.61/3.63	73.60/3.74	70.88/3.67	70.19/3.88	69.04/3.57 or 3.72
F	→3,6)-β-D-Galp-1→	103.28/4.53	75.22/3.32	81.50/3.52	74.47/3.23	70.42/3.49	69.45/3.64 or 3.68
G	→4)-α-GalpA-(1→	106.55/5.01	68.16/3.52	68.76/3.65	77.82/4.02	74.61/4.25	175.23/-
H	→3)-α-D-Rhap-(1→	100.86/5.08	79.26/4.24	70.18/3.87	73.45/3.83	66.24/3.98	16.66/1.18

3.7. Proposed Structure of CAP2-1

Integrating the results of results of multi-structure analysis, a putative structure for CAP2-1 was proposed in Figure 4. CAP2-1 consists of a backbone composed of →6)-β-D-Galp-(1→, →3,6)-β-D-Galp-(1→, and →4)-α-D-GalpA-(1→ residues. This backbone is substituted at O-3 positions by terminal α-D-Galp and →5)-α-L-Araf-(1→ residues. The side chains comprise terminal α-L-Araf, →5)-α-L-Araf-(1→, and →3,5)-α-L-Araf-(1→ units, with the latter further substituted at O-3 by additional terminal α-L-Araf residues.

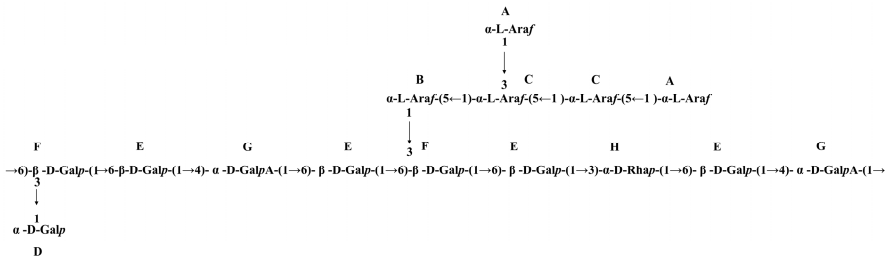


Figure 4. Proposed structure of CAP2-1.

These structural features indicate that CAP2-1 is a highly branched acidic arabinogalactan-type polysaccharide, consistent with its monosaccharide composition and degree of branching deduced from methylation data.

3.8. Antioxidant Activities of CAP2-1 and UCAP2-1

The antioxidant properties of CAP2-1 and its ultrasonic degradation product, UCAP2-1, were assessed based on their ability to scavenge DPPH, ABTS, and hydroxyl radicals, with Vc serving as a positive control. As illustrated in Figure 5, both CAP2-1 and UCAP2-1 exhibited concentration-dependent scavenging activity across all three assays. Notably, UCAP2-1 demonstrated consistently stronger radical scavenging capacity than CAP2-1, suggesting that ultrasonic depolymerization enhanced the antioxidant performance of the polysaccharide.

As illustrated in Figure 5a, at a concentration of 2.5 mg/mL, UCAP2-1 and CAP2-1 exhibited DPPH radical scavenging activities of 67.69% and 53.01%, respectively. UCAP2-1 displayed significantly higher activity ($p < 0.01$) than CAP2-1 in the concentration range of 0.5–2.5 mg/mL. DPPH radicals readily react with hydrogen-donating antioxidants to form stable non-radical products, making this assay a strong indicator of antioxidant capability [41].

A similar trend was observed in the ABTS radical scavenging assay in Figure 5b, at 2.5 mg/mL, UCAP2-1 achieved a scavenging rate of 82.07%, compared with 58.07% for CAP2-1, again demonstrating the superior antioxidant potential of the degraded fraction.

In Figure 5c, hydroxyl radical scavenging activity also showed notable differences between the two polysaccharides. At 2.5 mg/mL, UCAP2-1 and CAP2-1 exhibited scavenging activities of 53.07% and 37.30%, respectively. Across all tested concentrations above 0.5 mg/mL, UCAP2-1 maintained significantly higher scavenging activity ($p < 0.01$).

Collectively, these results indicate that UCAP2-1 possesses enhanced antioxidant properties compared with its polysaccharide CAP2-1. This enhancement in activity could be partially explained by its lower molecular weight, which has been widely associated with higher electron-donating capacity, better solubility, and improved accessibility to reactive sites. Specifically, polysaccharides with lower molecular weight generally exhibit enhanced antioxidant activity due to several factors. First, reduced chain length increases the availability of functional groups (hydroxyl and carboxyl groups) that can participate in electron or hydrogen donation, thereby improving free radical scavenging efficiency. Second, lower-molecular-weight polysaccharides typically display improved solubility and

dispersibility in aqueous systems, which facilitates their interaction with reactive oxygen species. Third, decreased steric hindrance and increased molecular flexibility enhance the accessibility of active sites, allowing more effective contact with free radicals. These combined effects provide a reasonable explanation for the higher antioxidant activity observed for UCAP2-1 compared to CAP2-1. Given the central role of DPPH, ABTS, and hydroxyl radicals in oxidative damage, the potent scavenging ability of UCAP2-1 suggests its potential as an effective antioxidant for mitigating oxidative stress, which contributes to aging, cancer, and various degenerative diseases [56]. While in vitro results establish a promising antioxidant profile for the polysaccharide, they constitute only a first-tier assessment. Variables such as limited bioavailability, extensive first-pass metabolism, and uneven tissue distribution can markedly diminish or modify activity in a living system. Consequently, the physiological significance of these findings remains to be confirmed through targeted in vivo investigations.

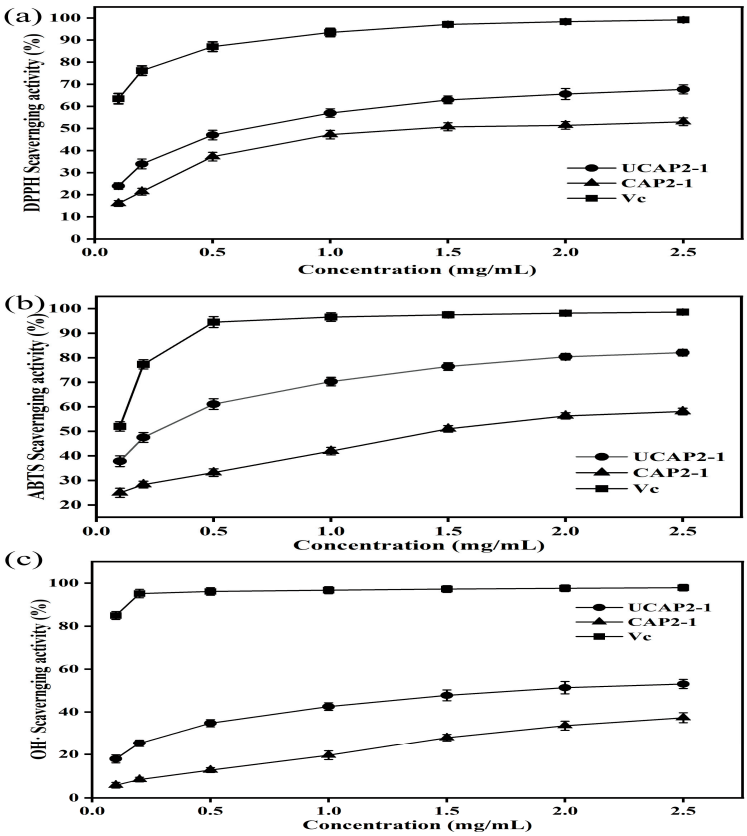


Figure 5. (**a**) DPPH radical scavenging activity; (**b**) ABTS radical scavenging activity; (**c**) Hydroxyl radical scavenging activity.

4. Conclusions

In the present work, a purified polysaccharide fraction (CAP2-1) was isolated from *C. auriculatum*. The polysaccharide CAP2-1 had an Mw of 184.17 kDa, with arabinose, galactose, and galacturonic acid as its dominant monosaccharide constituents. Structural analyses revealed that CAP2-1 is a highly branched acidic arabinogalactan-type polysaccharide with a backbone of →6)-β-D-Galp-(1→, →3,6)-β-D-Galp-(1→, and →4)-α-D-GalpA-(1→ residues, and side chains enriched in α-L-Araf units. Ultrasonic degradation produced UCAP2-1, a lower-molecular-weight derivative that displayed significantly enhanced scavenging activity toward DPPH, ABTS, and hydroxyl radicals. These findings suggest that reducing molecular weight can improve antioxidant properties, and that *C. auriculatum*—

particularly CAP2-1 and UCAP2-1—may have potential applications as natural antioxidant agents in functional food or pharmaceutical formulations.

Author Contributions: Conceptualization, H.Z. and M.M.N.; methodology, H.Z. and M.M.N.; software, H.Z. and M.M.N.; validation, H.Z., M.M.N., S.J., Y.S. and D.L.; formal analysis, H.Z., M.M.N., S.J., Y.S. and D.L.; investigation, H.Z. and M.M.N.; resources, C.L.; data curation, S.J., Y.S. and D.L.; writing—original draft preparation, H.Z.; writing—review and editing, H.Z. and C.L.; visualization, H.Z. supervision, M.M.N. and C.L.; project administration, C.L.; funding acquisition, C.L. All authors have read and agreed to the published version of the manuscript.

Funding: This research was funded by the Jiangsu Agriculture Science and Technology Innovation Fund, grant number CX (20) 2006.

Data Availability Statement: The original contributions presented in this study are included in the article. Further inquiries can be directed to the corresponding author.

Conflicts of Interest: The authors declare no conflicts of interest.

References

1. Van't Erve, T.J. Strategies to decrease oxidative stress biomarker levels in human medical conditions: A meta-analysis on 8-iso-prostaglandin F(2α). *Redox Biol.* **2018**, *17*, 284–296. [CrossRef]
2. Meng, Q.; Li, J.; Wang, C.; Shan, A. Biological function of resveratrol and its application in animal production: A review. *J. Anim. Sci. Biotechnol.* **2023**, *14*, 25. [CrossRef]
3. Clemente-Suárez, V.J.; Bustamante-Sanchez, A.; Rubio-Zarapuz, A.; Martín-Rodríguez, A.; Tornero-Aguilera, J.F.; Beltrán-Velasco, A.I. Biomimetic Strategies for Nutraceutical Delivery: Advances in Bionanomedicine for Enhanced Nutritional Health. *Biomimetics* **2025**, *10*, 426. [CrossRef]
4. Lee, W.E.; Genetzakis, E.; Figtree, G.A. Novel Strategies in the Early Detection and Treatment of Endothelial Cell-Specific Mitochondrial Dysfunction in Coronary Artery Disease. *Antioxidants* **2023**, *12*, 1359. [CrossRef]
5. Frandsen, J.R.; Narayanasamy, P. Neuroprotection through flavonoid: Enhancement of the glyoxalase pathway. *Redox Biol.* **2018**, *14*, 465–473. [CrossRef] [PubMed]
6. Bin Heyat, M.B.; Akhtar, F.; Abbas, S.J.; Al-Sarem, M.; Alqarafi, A.; Stalin, A.; Abbasi, R.; Muaad, A.Y.; Lai, D.; Wu, K. Wearable Flexible Electronics Based Cardiac Electrode for Researcher Mental Stress Detection System Using Machine Learning Models on Single Lead Electrocardiogram Signal. *Biosensors* **2022**, *12*, 427. [CrossRef]
7. Pathak, C.; Jaiswal, Y.K.; Vinayak, M. Queuine promotes antioxidant defence system by activating cellular antioxidant enzyme activities in cancer. *Biosci. Rep.* **2008**, *28*, 73–81. [CrossRef] [PubMed]
8. Yusri, N.M.; Chan, K.W.; Iqbal, S.; Ismail, M. Phenolic Content and Antioxidant Activity of *Hibiscus cannabinus* L. Seed Extracts after Sequential Solvent Extraction. *Molecules* **2012**, *17*, 12612–12621. [CrossRef]
9. Fernandes, P.A.R.; Coimbra, M.A. The antioxidant activity of polysaccharides: A structure-function relationship overview. *Carbohyd. Polym.* **2023**, *314*, 120965. [CrossRef] [PubMed]
10. Fu, Y.-P.; Li, C.-Y.; Peng, X.; Zou, Y.-F.; Rise, F.; Paulsen, B.S.; Wangensteen, H.; Inngjerdingen, K.T. Polysaccharides from *Aconitum carmichaelii* leaves: Structure, immunomodulatory and anti-inflammatory activities. *Carbohyd. Polym.* **2022**, *291*, 119655. [CrossRef]
11. Wang, N.; Zhang, X.; Wang, S.; Guo, Q.; Li, Z.; Liu, H.; Wang, C. Structural characterisation and immunomodulatory activity of polysaccharides from white asparagus skin. *Carbohyd. Polym.* **2020**, *227*, 115314. [CrossRef] [PubMed]
12. Zong, A.; Cao, H.; Wang, F. Anticancer polysaccharides from natural resources: A review of recent research. *Carbohyd. Polym.* **2012**, *90*, 1395–1410. [CrossRef]
13. Chen, F.; Huang, G. Antioxidant activity of polysaccharides from different sources of ginseng. *Int. J. Biol. Macromol.* **2019**, *125*, 906–908. [CrossRef]
14. Hu, Y.; Zhou, L.; Yang, J.; Bai, R.; Marchioni, E.; Zhao, M.; Zhou, L. Anti-inflammatory mechanism of *Houttuynia cordata* polysaccharides against ulcerative colitis based on multi-omics conjoint analysis. *Int. J. Biol. Macromol.* **2024**, *283*, 137311. [CrossRef]
15. Nie, C.; Zhu, P.; Ma, S.; Wang, M.; Hu, Y. Purification, characterization and immunomodulatory activity of polysaccharides from stem lettuce. *Carbohyd. Polym.* **2018**, *188*, 236–242. [CrossRef]
16. Wang, Z.; Zhou, X.; Shu, Z.; Zheng, Y.; Hu, X.; Zhang, P.; Huang, H.; Sheng, L.; Zhang, P.; Wang, Q.; et al. Regulation strategy, bioactivity, and physical property of plant and microbial polysaccharides based on molecular weight. *Int. J. Biol. Macromol.* **2023**, *244*, 125360. [CrossRef]

17. Zhou, H.; Fan, Z.; Li, Y.; Liu, X.; Wang, B.; Xing, J.; He, J.; Zheng, R.; Li, J. Structure–Antioxidant Activity Relationship of Polysaccharides Isolated by Microwave/Ultrasonic-Assisted Extraction from *Pleurotus ferulae*. *Antioxidants* **2025**, *14*, 91. [CrossRef] [PubMed]
18. Lo, T.C.-T.; Chang, C.A.; Chiu, K.-H.; Tsay, P.-K.; Jen, J.-F. Correlation evaluation of antioxidant properties on the monosaccharide components and glycosyl linkages of polysaccharide with different measuring methods. *Carbohyd. Polym.* **2011**, *86*, 320–327. [CrossRef]
19. Tang, Y.; He, X.; Liu, G.; Wei, Z.; Sheng, J.; Sun, J.; Li, C.; Xin, M.; Li, L.; Yi, P. Effects of different extraction methods on the structural, antioxidant and hypoglycemic properties of red pitaya stem polysaccharide. *Food Chem.* **2023**, *405*, 134804. [CrossRef]
20. Jing, Y.; Yan, M.; Zhang, H.; Liu, D.; Qiu, X.; Hu, B.; Zhang, D.; Zheng, Y.; Wu, L. Effects of Extraction Methods on the Physicochemical Properties and Biological Activities of Polysaccharides from *Polygonatum sibiricum*. *Foods* **2023**, *12*, 2088. [CrossRef] [PubMed]
21. Zhu, Y.; Feng, X.; Guo, J.; Wang, L.; Guo, X.; Zhu, X. A review of extraction, purification, structural properties and biological activities of legumes polysaccharides. *Front. Nutr.* **2022**, *9*, 1021448. [CrossRef]
22. Yuan, X.-H.; Tu, T.-T.; Mao, Y.-H.; Wang, Y.-C.; Huang, M.-Q.; Wang, L.; Luo, Y.; Wang, C.-X.; Qiu, S.-Y.; Deng, B.; et al. Characterization and bifidogenic effects of a low-molecular weight polysaccharide isolated from a Chinese herb, *Polygonatum kingianum* Coll. et Hemsl (Huangjing) rhizome. *Carbohyd. Polym.* **2026**, *373*, 124678. [CrossRef]
23. Guo, Q.; Huang, X.; Kang, J.; Ding, H.; Liu, Y.; Wang, N.; Cui, S.W. Immunomodulatory and antivirus activities of bioactive polysaccharides and structure-function relationship. *Bioact. Carbohydr. Diet. Fibre* **2022**, *27*, 100301. [CrossRef]
24. Chai, Z.; Huang, W.; Zhao, X.; Wu, H.; Zeng, X.; Li, C. Preparation, characterization, antioxidant activity and protective effect against cellular oxidative stress of polysaccharide from *Cynanchum auriculatum* Royle ex Wight. *Int. J. Biol. Macromol.* **2018**, *119*, 1068–1076. [CrossRef]
25. Wang, X.-J.; Li, Z.-L.; Lv, X.-H.; Zuo, Q.-Y.; Zhao, Y.-M.; Ding, Y.-F.; Pu, S.-B.; Qian, S.-H.; Peng, Y.-R. Anti-tumor evaluation and multiple analysis on different extracted fractions of the root of *Cynanchum auriculatum* Royle ex Wight. *J. Sep. Sci.* **2017**, *40*, 3054–3063. [CrossRef] [PubMed]
26. Nasiru, M.M.; Sun, Y.-E.; Zhao, L.; Bunhok, T.; Roth, C.M.; Sovath, S.; Pharith, H.; Wang, W.; Li, C. Isolation, Purification, and Antioxidant Activity of Polyphenols from *Cynanchum auriculatum* Royle ex Wight. *Separations* **2024**, *11*, 316. [CrossRef]
27. Wang, Y.; Han, J.; Yue, Y.; Wu, Y.; Zhang, W.; Xia, W.; Wu, M. Purification, structure identification and immune activity of a neutral polysaccharide from *Cynanchum auriculatum*. *Int. J. Biol. Macromol.* **2023**, *237*, 124142. [CrossRef] [PubMed]
28. Xu, Y.; Wu, C.; Wang, L.; Wu, S.; Chen, Y.; Ding, X.; Wang, L.; Yu, Y.; Du, W.; Zhang, Y.; et al. Phytochemical and chemotaxonomic investigations on the aerial parts of *Cynanchum auriculatum* Royle ex Wight. *Biochem. Syst. Ecol.* **2023**, *107*, 104609. [CrossRef]
29. Ding, X.; Wang, L.; Xu, Y.; Zheng, S.; Wang, S.; Wang, L.; Qin, M.; Wu, S.; Yu, Y.; Hong, J.; et al. Chemical constituents from the flowers of *Cynanchum auriculatum* Royle ex Wight. *Biochem. Syst. Ecol.* **2023**, *106*, 104562. [CrossRef]
30. Wu, Z.; Wang, Y.; Meng, X.; Wang, X.; Li, Z.; Qian, S.; Wei, Y.; Shu, L.; Ding, Y.; Wang, P.; et al. Total C-21 steroidal glycosides, isolated from the root tuber of *Cynanchum auriculatum* Royle ex Wight, attenuate hydrogen peroxide-induced oxidative injury and inflammation in L02 cells. *Int. J. Mol. Med.* **2018**, *42*, 3157–3170. [CrossRef]
31. Peng, Y.R.; Li, Y.B.; Liu, X.D.; Zhang, J.F.; Duan, J.A. Anti-tumor activity of C-21 steroidal glycosides from *Cynanchum auriculatum* Royle ex Wight. *Phytomedicine* **2008**, *15*, 1016–1020. [CrossRef]
32. Liu, Z.; Liu, Z.; Li, L.; Zhang, J.; Zhao, Q.; Lin, N.; Zhong, W.; Jiang, M. Immunomodulatory effects of the polysaccharide from *Sinonovacula constricta* on RAW264.7 macrophage cells. *Food Sci. Nutr.* **2022**, *10*, 1093–1102. [CrossRef]
33. DuBois, M.; Gilles, K.A.; Hamilton, J.K.; Rebers, P.A.; Smith, F. Colorimetric Method for Determination of Sugars and Related Substances. *Anal. Chem.* **1956**, *28*, 350–356. [CrossRef]
34. Li, Q.; Li, Y.; Niu, H.; Wang, E.; Jiao, L.; Li, H.; Wu, W. Structure Elucidation and Immunoactivity Study of *Armillaria mellea* Fruiting Body Polysaccharides. *Separations* **2024**, *11*, 3. [CrossRef]
35. Yang, L.; Zhang, H.; Zhao, Y.; Huang, J.; Zhu, D.; Wang, S.; Zhu, L.; Chen, L.; Xu, X.; Liu, H. Chemical structure, chain conformation and rheological properties of pectic polysaccharides from soy hulls. *Int. J. Biol. Macromol.* **2020**, *148*, 41–48. [CrossRef] [PubMed]
36. Li, B.; Dobruchowska, J.M.; Hoogenkamp, M.A.; Gerwig, G.J. Structural investigation of an extracellular polysaccharide produced by the cariogenic bacterium *Streptococcus mutans* strain UA159. *Carbohyd. Polym.* **2012**, *90*, 675–682. [CrossRef]
37. Tang, W.; Dong, M.; Wang, W.; Han, S.; Rui, X.; Chen, X.; Jiang, M.; Zhang, Q.; Wu, J.; Li, W. Structural characterization and antioxidant property of released exopolysaccharides from *Lactobacillus delbrueckii ssp*. bulgaricus SRFM-1. *Carbohyd. Polym.* **2017**, *173*, 654–664. [CrossRef]
38. Seedevi, P.; Moovendhan, M.; Sudharsan, S.; Sivasankar, P.; Sivakumar, L.; Vairamani, S.; Shanmugam, A. Isolation and chemical characteristics of rhamnose enriched polysaccharide from *Grateloupia lithophila*. *Carbohyd. Polym.* **2018**, *195*, 486–494. [CrossRef]
39. Zhu, Y.-M.; Pan, L.-C.; Zhang, L.-J.; Yin, Y.; Zhu, Z.-Y.; Sun, H.-Q.; Liu, C.-Y. Chemical structure and antioxidant activity of a polysaccharide from *Siraitia grosvenorii*. *Int. J. Biol. Macromol.* **2020**, *165*, 1900–1910. [CrossRef]

40. Xie, M.; Hu, B.; Wang, Y.; Zeng, X. Grafting of Gallic Acid onto Chitosan Enhances Antioxidant Activities and Alters Rheological Properties of the Copolymer. *J. Agr. Food Chem.* **2014**, *62*, 9128–9136. [CrossRef]
41. Li, C.; Huang, Q.; Fu, X.; Yue, X.-J.; Liu, R.H.; You, L.-J. Characterization, antioxidant and immunomodulatory activities of polysaccharides from *Prunella vulgaris* Linn. *Int. J. Biol. Macromol.* **2015**, *75*, 298–305. [CrossRef] [PubMed]
42. Jiang, J.; Kong, F.; Li, N.; Zhang, D.; Yan, C.; Lv, H. Purification, structural characterization and in vitro antioxidant activity of a novel polysaccharide from Boshuzhi. *Carbohyd. Polym.* **2016**, *147*, 365–371. [CrossRef]
43. Mkadmini Hammi, K.; Hammami, M.; Rihouey, C.; Le Cerf, D.; Ksouri, R.; Majdoub, H. Optimization extraction of polysaccharide from *Tunisian Zizyphus* lotus fruit by response surface methodology: Composition and antioxidant activity. *Food Chem.* **2016**, *212*, 476–484. [CrossRef]
44. Luo, Q.-L.; Tang, Z.-H.; Zhang, X.-F.; Zhong, Y.-H.; Yao, S.-Z.; Wang, L.-S.; Lin, C.-W.; Luo, X. Chemical properties and antioxidant activity of a water-soluble polysaccharide from *Dendrobium officinale*. *Int. J. Biol. Macromol.* **2016**, *89*, 219–227. [CrossRef]
45. Xu, Y.; Cai, F.; Yu, Z.; Zhang, L.; Li, X.; Yang, Y.; Liu, G. Optimisation of pressurised water extraction of polysaccharides from blackcurrant and its antioxidant activity. *Food Chem.* **2016**, *194*, 650–658. [CrossRef] [PubMed]
46. Zha, S.; Zhao, Q.; Chen, J.; Wang, L.; Zhang, G.; Zhang, H.; Zhao, B. Extraction, purification and antioxidant activities of the polysaccharides from maca (*Lepidium meyenii*). *Carbohyd. Polym.* **2014**, *111*, 584–587. [CrossRef] [PubMed]
47. Ye, Z.; Wang, W.; Yuan, Q.; Ye, H.; Sun, Y.; Zhang, H.; Zeng, X. Box–Behnken design for extraction optimization, characterization and in vitro antioxidant activity of *Cicer arietinum* L. hull polysaccharides. *Carbohyd. Polym.* **2016**, *147*, 354–364. [CrossRef]
48. Chen, Q.; Xue, G.; Ni, Q.; Wang, Y.; Gao, Q.; Zhang, Y.; Xu, G. Physicochemical and rheological characterization of pectin-rich polysaccharides from *Gardenia jasminoides* J. Ellis flower. *Food Sci. Nutr.* **2020**, *8*, 3335–3345. [CrossRef]
49. Wu, H.; Shu, L.; Liang, T.; Li, Y.; Liu, Y.; Zhong, X.; Xing, L.; Zeng, W.; Zhao, R.; Wang, X. Extraction optimization, physicochemical property, antioxidant activity, and α-glucosidase inhibitory effect of polysaccharides from lotus seedpods. *J. Sci. Food Agric.* **2022**, *102*, 4065–4078. [CrossRef]
50. Wang, Y.; Xiong, X.; Huang, G. Ultrasound-assisted extraction and analysis of maidenhairtree polysaccharides. *Ultrason. Sonochemistry* **2023**, *95*, 106395. [CrossRef]
51. Li, W.; Tang, W.; Ji, J.; Xia, X.; Rui, X.; Chen, X.; Jiang, M.; Zhou, J.; Dong, M. Characterization of a novel polysaccharide with anti-colon cancer activity from *Lactobacillus helveticus* MB2-1. *Carbohydr. Res.* **2015**, *411*, 6–14. [CrossRef]
52. Zhang, Y.; Zhou, T.; Wang, H.; Cui, Z.; Cheng, F.; Wang, K.-P. Structural characterization and in vitro anti-tumor activity of an acidic polysaccharide from *Angelica sinensis* (Oliv.) Diels. *Carbohyd. Polym.* **2016**, *147*, 401–408. [CrossRef]
53. Wang, X.; Zhang, H.; Wang, Z.; Bai, H. Optimization of ultrasonic-assisted alkaline extraction of polysaccharides from *Phellodendron amurense* Rupr. pollen using response surface methodology and its structure features. *RSC Adv.* **2015**, *5*, 106800–106808. [CrossRef]
54. Zhang, Q.; Xu, Y.; Zou, S.; Zhang, X.; Cao, K.; Fan, Q. Novel functional polysaccharides from *Radix Polygoni* Multiflori water extracted residue: Preliminary characterization and immunomodulatory activity. *Carbohyd. Polym.* **2016**, *137*, 625–631. [CrossRef] [PubMed]
55. Petersen, B.O.; Hindsgaul, O.; Paulsen, B.S.; Redondo, A.R.; Skovsted, I.C. Structural elucidation of the capsular polysaccharide from *Streptococcus pneumoniae* serotype 47A by NMR spectroscopy. *Carbohydr. Res.* **2014**, *386*, 62–67. [CrossRef] [PubMed]
56. Wu, Y.-T.; Huo, Y.-F.; Xu, L.; Xu, Y.-Y.; Wang, X.-L.; Zhou, T. Purification, characterization and antioxidant activity of polysaccharides from *Porphyra haitanensis*. *Int. J. Biol. Macromol.* **2020**, *165*, 2116–2125. [CrossRef]

Disclaimer/Publisher's Note: The statements, opinions and data contained in all publications are solely those of the individual author(s) and contributor(s) and not of MDPI and/or the editor(s). MDPI and/or the editor(s) disclaim responsibility for any injury to people or property resulting from any ideas, methods, instructions or products referred to in the content.